ISSN: 1410-8917
Jurnal Kimia Sains & Aplikasi
e-ISSN: 2597-9914

Jurnal Kimia Sains dan Aplikasi 25 (2) (2022): 71–78

Jurnal Kimia Sains dan Aplikasi
Journal of Scientific and Applied Chemistry

Journal homepage: http://ejournal.undip.ac.id/index.php/ksa

Catalytic hydrogenation of stearic acid to 1-octadecanol using supported bimetallic Pd–Sn(3.0)/γ–Al_2O_3 catalyst

Atina Sabila Azzahra [a,b], Elisa Hayati [a], Rodiansono [a,b*]

[a] Department of Chemistry, Faculty of Mathematics and Natural Sciences, Lambung Mangkurat University, Jl. A. Yani Km 36.0 Banjarbaru South Kalimantan, Indonesia
[b] Catalysis for Sustainable Energy and Environment (CATSuRe), Wetland-based Material Research Center, Lambung Mangkurat University, Banjarbaru South Kalimantan, Indonesia

*Corresponding author: rodiansono@ulm.ac.id (R. Rodiansono); Telp./Fax: +62-511-4773112

https://doi.org/10.14710/jksa.25.2.71-78

Article Info

Article history:

Received: 4th January 2022
Revised: 20th February 2022
Accepted: 24th February 2022
Online: 28th February 2022

Keywords:
Hydrogenation; Stearic Acid; 1– Octadecanol; Bimetallic Pd– Sn Catalyst

Abstract

Supported bimetallic palladium-tin catalyst on gamma-alumina (γ–Al_2O_3) (denoted as Pd–Sn(3.0)/γ–Al_2O_3; Pd = 5%wt and Pd/Sn molar ratio is 3.0) has been synthesized via the hydrothermal method at a temperature of 423 K for 24 h and reduced with H_2 at 673 K for 3 h. The XRD patterns of the samples showed typical diffraction peaks of support γ–Al_2O_3, metallic Pd, Sn, and Pd–Sn alloy phases. Diffraction peaks of metallic Pd were observed at 2θ = 39.8°; 46.6°; and 68.0°, which can be attributed to the Pd(111), Pd(200), and Pd(220), respectively, while the diffraction peaks at 2θ = 39.8° and 41.0° can be attributed to Pd_2Sn and Pd_3Sn_2, respectively, which may overlap with the Pd(111) species. The ammonia desorption and pyridine adsorption profiles showed Lewis and Brönsted acid sites. The specific surface area (S_{BET}) of Pd–Sn(3.0)/γ–Al_2O_3 catalyst was 117.83 m^2/g which is dominated by a micropore structure. The highest conversion of stearic acid was 99.1% with a yield of 1-octadecanol 43.2% was obtained at temperature 513 K, initial H_2 pressure of 2.0 MPa, a reaction time of 13 h, and in 2-propanol/water (4.0:1.0 v/v) solvent.

1. Introduction

The depletion of fossil fuel pushed numerous scientists to have great attention to searching for new energy resources and strategies to meet the increasing energy demand. The production of biodiesel has been intensively studied in recent years, in part due to political decisions to increase the use of biofuels, especially biodiesel palm oil-based. For instance, the Indonesian government has set a target energy level mixed with B50 to fossil diesel by 2025 [1]. On the other hand, diesel-like hydrocarbons, consisting of C16 to C18 carbon atoms, provide good fuel properties, such as viscosity, cloud point, and boiling point [2]. Long-chain hydrocarbons can be produced from fatty acids and their derivatives via hydrotreatment or catalytic hydrodeoxygenation (hydrogenation-dehydration-decarbonylation) [3]. The hydrogenation of fatty acids (e.g., stearic acid) to fatty alcohol using both heterogeneous and homogeneous catalysts is the crucial step in the transformation of biobased resources since fatty alcohol is widely used as the component of cosmetics, food ingredients, surfactant, plasticizer, lubricant, and intermediate of biofuel synthesis [4]. The use of homogeneous catalysts, such as Ru-Triphos complex [5] or iron-base PNP-pincer [6], showed high selectivity towards alcohols from the hydrogenation of carboxylic acids. However, homogeneous catalysts demonstrated much more selective than heterogeneous ones, with several drawbacks such as using expensive organic ligands, lack of reusability, and challenges associated with removing residual heavy metals in the isolated products. However, due to the high cost of the metal ligands used in these catalyst systems and problems associated with recycling the homogeneous catalysts, heterogeneous catalysts have proven to be more attractive choices for industrial applications [7].

Several attempts on the hydrogenation of stearic acid to 1-octadecanol using heterogeneous catalysts have

been reported previously [8]. The hydrogenation of fatty acids over a copper-chromite catalyst is commercially used to hydrogenate fatty acid esters to alcohols under severe conditions (2–50 MPa, 473–673 K) [9, 10, 11]. In addition, the presence of toxic chromium in the copper-chromite catalyst poses an environmental and health hazard. Therefore, the development of catalysts without using Cr and under milder reaction conditions has been attempted. Bimetallic platinum group metal (PGM) based catalysts such as Pt–Re/TiO_2 (2.0 MPa, 403 K) reported 61–90% selectivity to C_{10}–C_{18} fatty alcohols at 79–83% conversion [12]. The presence of co-promotor ReOx in Pd–ReOx/SiO_2, Rh–ReOx/SiO_2, and Ir–ReOx/SiO_2 catalysts (8.0 MPa, 413 K) enhanced the performance of Pd, Rh, and Ir catalysts to have 94–98% selectivity of 1-octadecanol at 100% conversion [13]. However, noble metal-based catalysts and low substrate loading are not economical and have less viability in upgrading the biomass-derived platform industry. Therefore, alternative economic and eco-friendly heterogeneous catalysts that would ensure the preferred hydrogenation of the carboxylic acids (fatty acid) to fatty alcohol are highly desired.

The electropositive metals such as tin (Sn), indium (In) of iron (Fe) have been widely used as co-promotor for Ru, Pd, or Ni-based bimetallic catalysts. Toba *et al.* reported that 2wt% Ru-4.7wt% Sn/Al_2O_3 showed high selectivity toward alcohols (89.4%) at 97.3% adipic acid conversion at 513 K and 6.5 MPa of H_2 [14]. Bimetallic Ni–Sn alloy supported on TiO_2 (Ni-Sn(1.5)/TiO_2) catalyst showed a high yield of lauryl alcohol at (97%) at >99% conversion of lauric acid at 433 K, 3.0 MPa H_2 for 20 h [15]. Damayanti *et al.* reported using bimetallic Pd-Fe/TiO_2 catalyst for the hydrogenation of levulinic acid (LA) to γ-valerolactone (GVL) at 443 K, 3.0 MPa H_2 for 7 h. The obtained yield of GVL over Ru-Fe/TiO_2 was 52.4%, much higher than that of Pd/TiO_2 (22.7%) [16]. Most recently, supported bimetallic Pd-Sn(*x*)/C catalysts demonstrated a high yield of 1-octadecanol (73.2%) at 100% conversion of stearic acid. The high selectivity of alcohols over Pd-Sn(1.5)/C catalyst can be attributed to the formation of bimetallic Pd-Sn alloy phases (e.g., Pd_3Sn and Pd_3Sn_2) as obviously depicted by XRD analysis [17].

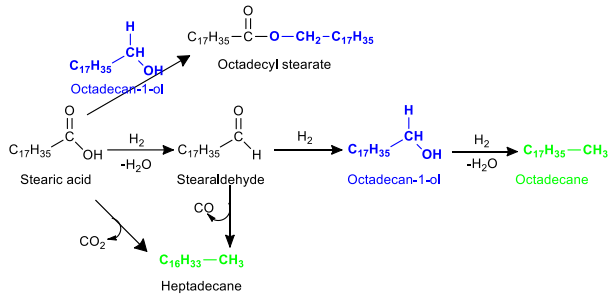

Scheme 1. Conceived reaction routes for the catalytic transformation of stearic acid using heterogeneous catalysts

In this paper, an extended investigation on the gamma-alumina supported bimetallic palladium-tin catalysts (denoted as Pd-Sn(3.0)/γ–Al_2O_3; Pd = 5%wt and Pd/Sn molar ratio is 3.0) for the hydrogenation of stearic acid to 1-octadecanol under mild reaction conditions has been investigated. The current results showed that Pd-Sn(3.0)/γ–Al_2O_3 catalyst showed the highest conversion of stearic acid (99.1%) and 1-octadecanol yield (43.2%), which were higher than that of other supported Pd-Sn catalysts under the applied reaction conditions.

2. Materials and Methods

2.1. Materials

Palladium(II) acetate ($Pd(CH_3COO)_2$; 98%) and tin(II) chloride dihydrate ($SnCl_2{\cdot}2H_2O$; 99%) were purchased from WAKO Pure Chemical Industries, Ltd), Y-Zeolit , HZSM-5 Si/Al 85 (S_{BET} = 417 m^2/g; Vp = 0.2252 cm^3/g; pore diameter = 3.64 nm), Nb_2O_5 dan TiO_2 anatase were purchased and used as received from WAKO Pure Chemical Industries, Ltd. γ–Al_2O_3 (S_{BET} = 100 m^2/g) was purchased from Japan Aerosil Co. Ethanol (96.0%; Merck Millipore), ethylene glycol (EG) (99.5%; Merck Millipore), $NaBH_4$ (95.0%; Tokyo Chemical Industry (TCI)), NaOH (99.0%; Merck Millipore). Stearic acid (98%; TCI), 1-octadecanol (98%; TCI), heptadecane (99%; TCI), dodecane (99%, TCI) were purchased from Tokyo Chemical Industries Co. (TCI).

2.2. Catalyst preparation

A typical procedure of the synthesis of supported bimetallic Pd–Sn(3.0)/γ–Al_2O_3 (Pd = 5%b/b and Pd/Sn feeding molar ratio of 3.0) catalyst is described as follows [15, 17]: $Pd(CH_3COO)_2$ (0.4613 mmol) was dissolved in deionized water (denoted as solution A), and $SnCl_2{\cdot}2H_2O$ (0.1537 mmol) was dissolved in ethanol/ethylene glycol (20:10 v/v mL) (denoted as solution B) at room temperature. Solutions A and B and 1.0 g of support (γ–Al_2O_3) were mixed at room temperature; the temperature was subsequently raised to 323 K, and the mixture was gently stirred for 12 h. The mixture was adjusted to pH 12 by dropwise an aqueous solution of NaOH (3.1 M or 6.0 M) and placed into a sealed-Teflon autoclave for the hydrothermal reaction at 423 K for 24 h. The resulting black precipitate was filtered, washed with distilled water, and then dried under vacuum overnight. Prior to the catalytic reaction, the obtained black powder was reduced with hydrogen (H_2) gas at 673 K for 3 h [18]. Bimetallic Pd–Sn supported on Y-Zeolite, HZSM-5 Si/Al = 8, Nb_2O_5 dan TiO_2 catalysts were also synthesized using a similar procedure.

2.3. Characterizations

The prepared catalysts were characterized by powder X-ray diffraction on a RIGAKU MINIFLEX 600 instrument using monochromatic CuKα radiation (λ=0.15418 nm). It was operated at 40 kV and 20 mA with a step width of 0.02° and a scan speed of 5° min^{-1}. According to Scherrer's equation, the mean crystallite size of Ni was calculated from the full width at half maximum (FWHM) of the Pd(111) diffraction peak.

Nitrogen adsorption isotherms at 77 K were measured by Belsorp Max (BEL Japan). The samples were degassed at 473 K for 2 h to remove physisorbed gases prior to the measurement. The amount of nitrogen adsorbed onto the samples was used to calculate the specific surface area employing the BET equation. The

total pore volume was estimated to be the liquid volume of nitrogen at a relative pressure of about 0.995. The Barrett–Joyner–Halenda (BJH) approach was used to calculate desorption data's total pore volume and size distribution [19].

The temperature-programmed desorption of ammonia (NH_3-TPD) was carried out on a Belsorp Max (BEL Japan). The samples were degassed at an elevated temperature of 373–473 K for 2 h to remove physisorbed gases prior to the measurement. The temperature was then kept at 473 K for 2 h while flushed with helium gas. NH_3 gas (80% balanced NH_3 and 20% He) was introduced at 373 K for 30 minutes, then evacuated by helium gas to remove the physisorbed for 30 minutes. Finally, temperature-programmed desorption was carried out at 273–1073 K temperatures, and TCD monitored the desorbed NH_3.

Attenuated total reflection-Fourier transformed infrared (ATR-FTIR) analysis was performed on a Diamond Bruker spectrometer with a resolution of 2 cm^{-1} and a scanning number of 36. A 20 mg sample in powder form was degassed under vacuum (10^{-3} Pa) for 1 h at 423 K in the TAIATSU techno *with glass-fitted inside*. Then, it was cooled to room temperature, and the initial background spectrum was recorded. After the sample was exposed to pyridine vapor under vacuum for 60 minutes and overnight, followed by removal of the excessive pyridine at 323 K for 0.5 h, then measured by ATR-FTIR.

2.4. Catalytic reactions

A typical procedure for hydrogenation of stearic acid was described as follows: catalyst (0.05 g), stearic acid (0.2844 g; 1.0 mmol), 2-propanol:H_2O (5 mL; 4.0:1.0 v/v) as solvent were placed into a glass reaction tube, which fitted inside a stainless steel reactor. After H_2 was introduced into the reactor with an initial H_2 pressure of 2.0 MPa at room temperature, the reactor's temperature was increased to 513 K using an electric furnace, 800 rpm. After 13 h, at room temperature, the internal standard of dodecane was added, and the conversion of stearic acid and the yield of 1-octadecanol were determined by GC analysis. The Pd–Sn/γ–Al_2O_3 catalyst was easily separated using simple centrifugation or filtration.

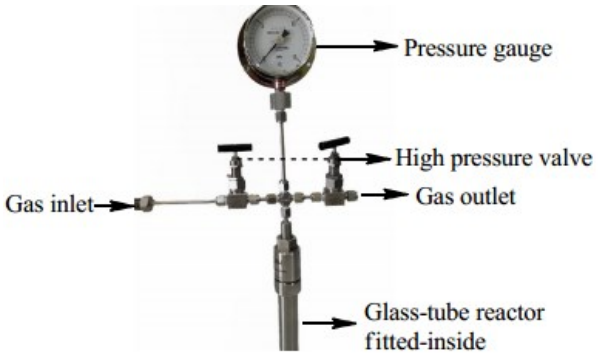

Figure 1. Typical batch system reactor of TAIATSU techno *with glass-fitted inside* (volume: 30 mL, max. 35 MPa, 300°C)

2.5. Product Analysis

GC analysis of the reactant (stearic acid) and products (1-octadecanol, ester, and heptadecane) was performed on a Perkin Elmer AutoSystem XL equipped with a flame ionization detector and Thermo Scientific (0.25 mm × 15 m × 0.25 µm) capillary column. It was operated under the following conditions: injector and detector temperatures (523 K); airflow (450 mL/min); H_2 flow (45 mL/min); N_2 flow (14 mL/min); and a split ratio of 50:1. The temperature column has been set gradually into two steps (first: 373–493 K (ramping of 20 K/min) and second: 493–573 K (ramping of 18 K/min). Gas chromatography-mass spectrometry (GC-MS) was performed on a Shimadzu GC-17 equipped with a thermal conductivity detector and an RT-βDEXsm capillary column. The products were confirmed by comparing their GC retention time and mass spectra with those of authentic samples.

The conversion, yield, and selectivity of the products were calculated according to the following equations:

Conversion:

$$\frac{\text{introduced mol reactant } (F_0) - \text{remained mol reactant } (F_t)}{\text{introduced mol reactant } (F_0)} \text{ x } 100\%$$

Yield:

$$\frac{\text{mol product}}{\text{consumed mol reactant } (\Delta F)} \text{ x } 100\%$$

Selectivity:

$$\frac{\text{mol product}}{\text{total mol products}} \text{ x } 100\%$$

F_o is the introduced mol reactant (stearic acid), F_t is the remaining mol reactant, and ΔF is the consumed mol reactant (introduced mol reactant-remained mol reactant), which are all obtained from GC analysis using a standard internal technique.

3. Results and Discussion

3.1. Catalysts characterization

The N_2-adsorption/desorption and pore distribution (Horvath-Kawazoe (HK) method) of the synthesized bimetallic Pd–Sn(3.0)/γ–Al_2O_3 catalyst were performed, and the profiles are shown in Figure 2.

The hysteresis loop of adsorption/desorption of the synthesized bimetallic Pd–Sn(3.0)/γ–Al_2O_3 sample is very similar to that of IV type, which indicates the strong interaction between the molecule adsorbate and catalyst surface. The formation of the hysteresis loop also indicated the condensation of molecule adsorbate during the desorption of N_2 gas [20] (Figure 2(a)). The plot of the volume of adsorbed-N_2 versus pore distribution using the Horvath-Kawazoe (HK) method was performed to determine the pore size distribution of the synthesized catalysts, as shown in Figure 2(b). The pore size distribution was ≥1.16 nm after reduction with H_2 at 400°C. However, there is no clear evidence for the change in the pore size distribution towards small pore sizes or big pore sizes after introducing the Pd–Sn species or thermal activation using N_2 or H_2 at 400°C.

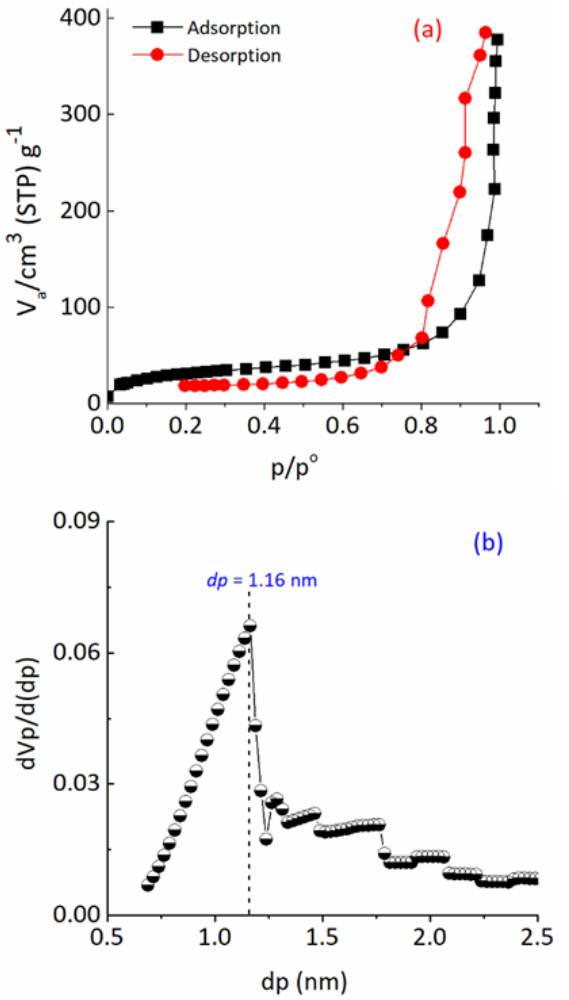

Figure 2. (a) Typical N_2-adsorption/desorption profiles and (b) pore distribution profiles using Hovarth-Kawazoe (HK) of the synthesized Pd–Sn(3.0)/γ–Al_2O_3 catalyst

To validate the pore structure (micropore and mesopore area) and the possible adsorption of the catalyst sample, the t-plot and α-plot techniques were performed. The results are shown in Figure 3. The frontline of t-plot profiles showed that the sample has mainly micropore structure (≤ 1.0 nm) (Figure 3(a)), whereas the frontline of α-plot profiles showed both the micropore and the mesopore structures (≥ 2.0 nm) (Figure 3(b)). The pore size at ≥ 2.0 nm was observed when the volume of N_2 gas increased up to 200 cm³/g. Therefore, it can be concluded that the synthesized Pd–Sn(3.0)/γ-Al_2O_3 catalyst has both micro and mesopore structures [21].

Table 1. Physicochemical properties of supported bimetallic Pd–Sn(3.0)/γ–Al_2O_3 catalyst

Entry	S_{BET}/ m² g⁻¹	SA(t-plot) /m² g⁻¹		SA(α–plot) /m² g⁻¹		Pore size distribution/nm		Pore vol./cm³g⁻¹	
		Micro.	Meso.	Micro.	Meso.	BJH	HK	BET	BJH
1	117.83	90.8	89.2	62.4	3.4	1.21	1.16	0.55	0.53
2	637	-	-	-	-	-	0.94	0.49	-

Table 1 summarized the porosity properties (specific surface area (S_{BET}), micro and mesopore surface area, pore-volume, and pore size distributions (entry 1). Pd–Sn(3.0)/γ–Al_2O_3 catalyst has similarity with Pd–Sn(3.0)/C, which has both microstructures on the surface. The differences are Pd–Sn(3.0)/C has a higher surface area than Pd–Sn(3.0)/γ–Al_2O_3 with pore size distribution and pore volume smaller than Pd–Sn(3.0)/γ–Al_2O_3 (entry 2) [17].

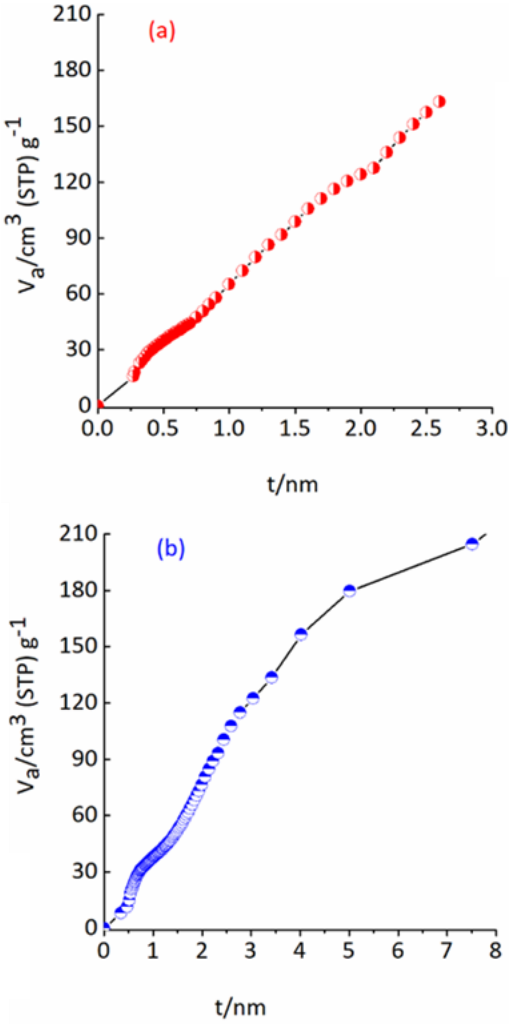

Figure 3. (a) t-plot profiles and (b) alpha (α)-plot profiles of the synthesized Pd–Sn(3.0)/γ-Al_2O_3 catalyst

The total acid site density was derived from the amounts of desorbed ammonia, which were formally divided into three temperature regions to denote three types of acid sites: (1) weak acid sites, ranging from 373 to 573 K, (2) moderate acid strength, ranging from 573 to 823 K, and (3) high acid strength, ranging from 823 to 1023 K [22, 23, 24, 25]. The results of temperature-programmed desorption of ammonia (NH_3-TPD) and ATR-FTIR of pyridine adsorption are shown in Figure 4 and Table 2. Pd–Sn(3.0)/γ–Al_2O_3 catalyst has weak and strong acid sites with amount acid sites 11 µmol/g and 380 µmol/g, respectively. ATR-FTIR analysis of adsorbed pyridine also confirmed that the Pd–Sn(3.0)/γ–Al_2O_3 catalyst has both Lewis and Brönsted acid sites, suggesting that the effect of total acidity might play an essential role during the selective hydrogenation of stearic acid to 1-octadecanol (stearyl alcohol) under the current operating conditions.

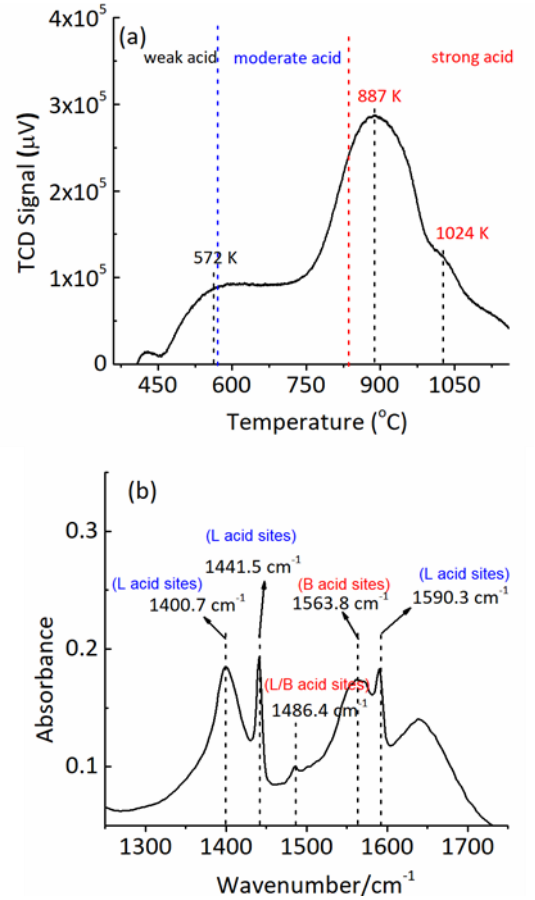

Figure 4. (a) Temperature-programmed desorption of ammonia (NH_3-TPD) profiles and (b) ATR-FTIR spectra of adsorbed pyridine on the synthesized Pd–Sn(3.0)/γ–Al_2O_3 catalyst

Table 2. Physicochemical properties of supported bimetallic Pd-Sn(3.0)/γ–Al_2O_3 catalyst

NH_3-TPD (Acidity/μmol/g)				Pyridine adsorption (band position)	
Weak (373-623 K)	Moderate (623-823 K)	Strong (823-1023 K)	Total acidity/ μmol/g	Lewis (L) acid	Brönsted (B) acid
11	-	380	391	1400.7 cm^{-1} 1441.5 cm^{-1} 1590.3 cm^{-1}	1486.4 cm^{-1} 1563.8 cm^{-1}

[a]Total acid sites were derived from NH_3-TPD data

Figure 5 shows the XRD patterns of commercial γ–Al_2O_3 support, as prepared and pre-reduced bimetallic Pd–Sn(3.0)/γ–Al_2O_3 catalyst. The commercial γ–Al_2O_3 support exhibited a typical diffraction peak of crystalline of γ–Al_2O_3 support (Figure 5(a)). In the case of Pd–Sn(3.0)/γ–Al_2O_3 catalyst, the typical diffraction peaks at 2θ = 14°; 32.9°; 34.2°; dan 65.9° were clearly observed, which can be attributed to the tin oxide (SnO) (JCPDS#04-673), Sn (101) (JCPDS#18-1380) and SnO_2(301) (JCPDS#41-1445) phases, respectively (Figure 5(a)(b)) [7, 26, 27]. A high intensity of the diffraction peak at 2θ = 40.2° of Pd–Sn(3.0)/γ–Al_2O_3 sample after reduction with H_2 at 673 K that can be suggested due to the modified surface structure of Pd(111) in the presence of Sn promoter either to form surface bimetallic or alloy Pd–Sn (Pd_2Sn species; JCPDS#007-1070) (Figure 5(c)) [28, 29, 30].

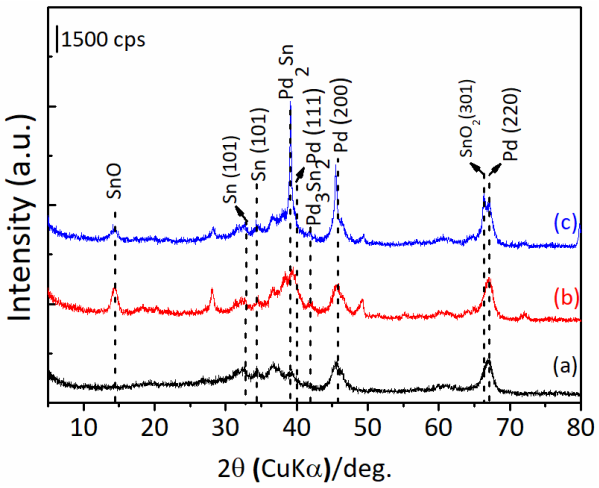

Figure 5. XRD patterns of (a) γ–Al_2O_3 support, (b) as-prepared, and (c) H_2-reduced Pd–Sn(3.0)/γ–Al_2O_3 catalyst at 673 K for 3 h

3.2. Screening of catalyst

The catalytic reaction of stearic acid using various palladium-based catalysts was performed in 2-propanol/H_2O (4.0:1.0 v/v) solvent, 513 K, 2.0 MPa H_2 for 7 h, and the results are summarized in Table 3. The catalytic conversion of stearic acid using various supported bimetallic Pd–Sn catalysts was investigated, and the results were also shown in Table 3. The conversion of stearic acid was varied at 47–92%, the maximum yield of 1-octadecanol was only 6.5% at a conversion of 91.7%, obtained over Pd–Sn(3.0)/HZM-5 catalyst (entries 1–4). The currently obtained yields of 1-octadecanol using Pd–Sn(3.0) supported on various metal oxides and zeolites were much lower than that of supported Pd–Sn(1.5) catalysts under similar reaction conditions as recently reported by Rodiansono *et al.* [17]. By using Pd–Sn(3.0)/γ–Al_2O_3 catalyst, a remarkably high yield of 1-octadecanol (22.7%) at 94.7% conversion of stearic acid was achieved (entry 5).

In order to understand the reaction profiles, the hydrogenation of stearic acid in the presence of a Pd–Sn(3.0)/γ–Al_2O_3 catalyst at different reaction times was carried out. At an earlier reaction time of 1 h, the conversion of stearic acid was only 12.9% without forming a hydrogenated product of 1-octadecanol (entry 6). The yield of 1-octadecanol significantly increased to 12.5% (at 84.4% conversion of stearic acid) when the reaction time of 5 h was applied. Further prolonged reaction time to 13 h, the conversion of stearic acid was nearly 100%, and a maximum yield of 1-octadecanol (43.2%) was obtained (entry 8). To confirm the importance of bimetallic Pd-Sn instead of monometallic Pd catalyst, the catalytic reaction over Pd/γ–Al_2O_3 gave 81.3% conversion of stearic acid. The products were distributed to 1-octadecanol (2.1%), ester (isopropyl stearate) (26.5%), and others (52.7%) after 13 h (entry 9). These results suggested that the presence of Sn in Pd–Sn(3.0)/γ–Al_2O_3 might enhance the selectivity product of 1-octadecanol by inhibiting the decarboxylation reaction compared to the monometallic Pd/γ–Al_2O_3 catalyst [31, 32].

The conversion of stearic acid using Ni–FeO_x and Ru_3Sn_7/SiO_2 catalysts were reported as 75–100%. The 20% and 99% yields were obtained using Ni–FeO_x and Ru_3Sn_7/SiO_2 catalysts, respectively (entry 10–11). Although both catalysts showed good performance, these catalysts required harsher reaction conditions than the Pd-Sn/γ–Al_2O_3 catalyst.

Table 3. Results of catalyst screening for hydrogenation of stearic acid to 1-octadecanol

Entry	Catalyst[a]	Reaction time (h)	Conv.[d] (%)	Yield[d] (%)		
				1-Octadecanol	Ester	Others[e]
1	Pd–Sn(3.0)/Nb_2O_5	7	79.2	3.4	72.4	3.4
2	Pd–Sn(3.0)/TiO_2	7	47.9	2.8	42.2	2.9
3	Pd–Sn(3.0)/Y-Zeolite	7	46.0	1.7	39.0	5.3
4	Pd–Sn(3.0)/HZSM-5	7	91.7	6.5	80.4	5.8
5	Pd–Sn(3.0)/γ–Al_2O_3	7	94.7	22.7	60.6	11.4
6	Pd–Sn(3.0)/γ–Al_2O_3	1	12.9	0.0	1.0	11.9
7	Pd–Sn(3.0)/γ–Al_2O_3	5	84.4	12.5	65.3	6.6
8	Pd–Sn(3.0)/γ–Al_2O_3	13	99.1	43.2	45.0	10.9
9	Pd/γ–Al_2O_3	13	81.3	2.1	26.5	52.7
10[b]	Ni–FeO_x	20	75	20	-	-
11[c]	Ru_3Sn_7/SiO_2	2–4	100	99	-	-

Reaction conditions: catalyst (0.05 g); stearic acid (0.2844 g; 1.0 mmol); solvent (2-propanol/H_2O; 5.0 mL; 4.0:1.0 v/v); temperature 513 K; initial H_2 pressure (2.0 MPa); reaction time (7 h). [a]The value in the parenthesis is the Pd/Sn molar ratio; based on the amount of metal salt precursor. [b]Reaction conditions: catalyst (0.1 g); stearic acid (0.3 g); solvent (1.4-dioxane 30 mL); temperature 523 K; initial H_2 pressure (5.0 MPa) [17]. [c]Reaction conditions: catalyst (0.2 g); solvent (dodecane 80 mL); temperature 513 K; initial H_2 pressure (4.0 MPa) [7]. [d]Conversion was determined by GC using a standard internal technique. [d]Yields were determined by GC using GC area ratio according to GC-MS data. [d]Others were included hydrocarbon and unidentified products based on the GC-MS analysis data [17].

3.3. Effect of reaction temperature

The effect of reaction temperature on the conversion and product distribution in the catalytic conversion of stearic acid over bimetallic Pd–Sn(3.0)/γ–Al_2O_3 catalyst was investigated. As shown in Table 4, at the reaction temperature of 433 K, the conversion of stearic acid was 22.8%, and the products were distributed to 1-octadecanol (1.1%), ester (19.1%), and other products (2.6%) (entry 1). The increase in reaction temperature to 473 K increased stearic acid conversion (49.6%). However, the yield of 1-octadecanol was remained low (2.0%), whereas the formation of ester and other products increased significantly (entry 2). When the reaction temperature was increased to 513 K, high conversion of stearic acid (94.7%) with remained low 1-octadecanol yield (22.7%) was obtained (entry 3).

In these reaction conditions, the yield of ester (mainly contains isopropyl stearate) and others were still much higher than that of Pd–Sn(1.5)/γ–Al_2O_3 catalysts (entry 4). The hydrogenation of fatty acid using Pd-based catalysts required a co-promotor to enhance alcohol selectivity and inhibit the decarboxylation reaction, producing alkanes as the main products [13, 33]. This result suggested that the further reaction of the formed alcohol to another side product occurred during the hydrogenation of stearic acid, as indicated by the number of others.

Table 4. Effect of reaction temperature on conversion and product distribution in the hydrogenation of stearic acid using Pd–Sn(3.0)/γ–Al_2O_3

Entry	Temp. (K)	Conv.[a] (%)	Yield[b] (%)		
			1-octadecanol	Ester	Others[c]
1	433	22.8	1.1	19.1	2.6
2	473	49.6	2.0	41.7	5.9
3	513	94.7	22.7	60.6	11.4
4[d]	513	84.4	32.5	45.3	6.6

Reaction conditions: catalyst (0.05 g); stearic acid (0.2844 g; 1.0 mmol); solvent (2-propanol/H_2O (5.0 mL; 4.0:1.0 v/v); 513 K; initial H_2 pressure (3.0 MPa); reaction time (7 h). [a]Conversion was determined by GC using a standard internal technique. [b]Yields were determined by GC using GC area ratio according to GC-MS data. [c]Others were included hydrocarbon and unidentified products based on the GC-MS analysis data. [d]Data was taken from the cited reference of Rodiansono *et al.* [17].

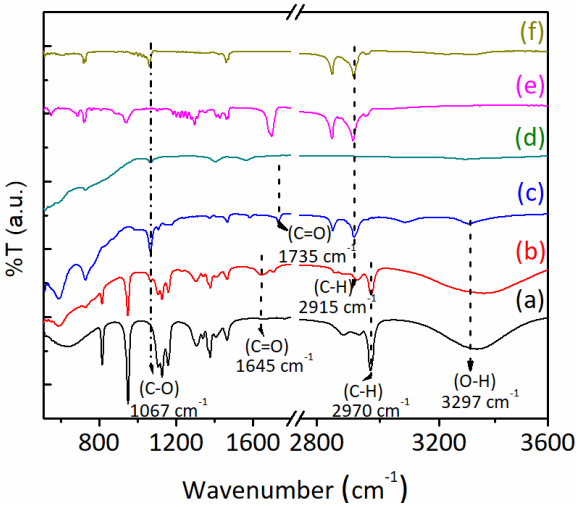

Figure 6. ATR-FTIR spectra of fresh and recovered catalysts and their possible interaction between Pd–Sn(3.0)/γ–Al_2O_3 catalyst and the molecular reactant of stearic acid. (a) 2-propanol; (b) wetted recovered catalyst; (c) dried recovered catalyst; (d) freshly activated catalyst; (e) stearic acid; and (f)1-octadecanol

ATR-IR analysis of the recovered catalyst was carried out, and the results are shown in Figure 6. Two absorption peaks at wavenumber (υ) 1067 cm^{-1} and 3297 cm^{-1} can be assigned as C–O and O–H stretching, respectively. The presence of a sharp peak at 2970 cm^{-1}, which can be assigned as $–CH_2$, was also clearly observed. A small peak at 1735 cm^{-1} was observed in Figure 6b, which can be

attributed to the C=O functional group of the remaining stearic acid reactant.

4. Conclusion

We described the selective hydrogenation of stearic acid to corresponding alcohol using Pd–Sn(3.0)/γ–Al_2O_3 catalyst under mild reaction conditions. The highest yield of stearyl alcohol (1-octadecanol) (up to 43.2%) at 99.1% conversion of stearic acid at temperature 240°C, initial H_2 pressure of 2.0 MPa, a reaction time of 13 h, and in 2-propanol/water (4.0:1.0 v/v) solvent. Under the current reaction conditions, the main product obtained over Pd–Sn(3.0)/γ–Al_2O_3 catalyst was ester stearate (isopropyl stearate) and others. The high yield of ester and other products may be due to the high acidity of catalyst as indicated by NH_3-TPD and ATR-FTIR pyridine adsorption analysis.

Acknowledgments

The authors acknowledge the BPDP Kelapa Sawit, Ministry of Finance, the RISET DASAR & Hibah Berbasis Kompetensi (HIKOM) FY 2018-2020, and the RISET DASAR FY 2019-2021 (contract number DIPA-042.06-1.401516/2020) from the Ministry of Research, Technology, and Higher Education, which all financially supported this work.

References

[1] BPDP, Roadmap Penelitian dan Pengembangan Sawit, (2021)

[2] Wayne K. Craig, Douglas W. Soveran, *Production of hydrocarbons with a relatively high cetane rating*, Canada Minister of Energy Mines and Resources, The United States, 1991

[3] Siswati Lestari, Päivi Mäki - Arvela, Jorge Beltramini, GQ Max Lu, Dmitry Yu Murzin, Transforming triglycerides and fatty acids into biofuels, *ChemSusChem: Chemistry & Sustainability Energy & Materials*, 2, 12, (2009), 1109-1119 https://doi.org/10.1002/cssc.200900107

[4] Yasuyuki Takeda, Masazumi Tamura, Yoshinao Nakagawa, Kazu Okumura, Keiichi Tomishige, Characterization of Re–Pd/SiO_2 catalysts for hydrogenation of stearic acid, *ACS Catalysis*, 5, 11, (2015), 7034-7047 https://doi.org/10.1021/acscatal.5b01054

[5] Thorsten vom Stein, Markus Meuresch, Dominik Limper, Marc Schmitz, Markus Hölscher, Jacorien Coetzee, David J. Cole-Hamilton, Jürgen Klankermayer, Walter Leitner, Highly versatile catalytic hydrogenation of carboxylic and carbonic acid derivatives using a Ru-triphos complex: molecular control over selectivity and substrate scope, *Journal of the American Chemical Society*, 136, 38, (2014), 13217-13225 https://doi.org/10.1021/ja506023f

[6] Sumit Chakraborty, Huiguang Dai, Papri Bhattacharya, Neil T. Fairweather, Michael S. Gibson, Jeanette A. Krause, Hairong Guan, Iron-based catalysts for the hydrogenation of esters to alcohols, *Journal of the American Chemical Society*, 136, 22, (2014), 7869-7872 https://doi.org/10.1021/ja5040349

[7] Zhicheng Luo, Qiming Bing, Jiechen Kong, Jing-yao Liu, Chen Zhao, Mechanism of supported Ru_3Sn_7 nanocluster-catalyzed selective hydrogenation of coconut oil to fatty alcohols, *Catalysis Science & Technology*, 8, 5, (2018), 1322-1332 https://doi.org/10.1039/C8CY00037A

[8] James Pritchard, Georgy A. Filonenko, Robbert Van Putten, Emiel J. M. Hensen, Evgeny A. Pidko, Heterogeneous and homogeneous catalysis for the hydrogenation of carboxylic acid derivatives: history, advances and future directions, *Chemical Society Reviews*, 44, 11, (2015), 3808-3833 https://doi.org/10.1039/C5CS00038F

[9] Karl Folkers, Homer Adkins, The catalytic hydrogenation of esters to alcohols. II, *Journal of the American Chemical Society*, 54, 3, (1932), 1145-1154 https://doi.org/10.1021/ja01342a043

[10] Ross D. Rieke, Deepak S. Thakur, Brian D. Roberts, Geoffrey T. White, Fatty methyl ester hydrogenation to fatty alcohol part I: correlation between catalyst properties and activity/selectivity, *Journal of the American Oil Chemists' Society*, 74, 4, (1997), 333-339 https://doi.org/10.1007/s11746-997-0088-y

[11] Ross D. Rieke, Deepak S. Thakur, Brian D. Roberts, Geoffrey T. White, Fatty methyl ester hydrogenation to fatty alcohol part II: process issues, *Journal of the American Oil Chemists' Society*, 74, 4, (1997), 341-345 https://doi.org/10.1007/s11746-997-0089-x

[12] Haresh G. Manyar, Cristina Paun, Rashidah Pilus, David W. Rooney, Jillian M. Thompson, Christopher Hardacre, Highly selective and efficient hydrogenation of carboxylic acids to alcohols using titania supported Pt catalysts, *Chemical Communications*, 46, 34, (2010), 6279-6281 https://doi.org/10.1039/C0CC01365J

[13] Yasuyuki Takeda, Yoshinao Nakagawa, Keiichi Tomishige, Selective hydrogenation of higher saturated carboxylic acids to alcohols using a ReO_x–Pd/SiO_2 catalyst, *Catalysis Science & Technology*, 2, 11, (2012), 2221-2223 https://doi.org/10.1039/C2CY20302B

[14] Makoto Toba, Shin-ichi Tanaka, Shu-ichi Niwa, Fujio Mizukami, Zsuzsanna Koppány, László Guczi, Kien-Yoo Cheah, Thin-Sue Tang, Synthesis of alcohols and diols by hydrogenation of carboxylic acids and esters over Ru–Sn–Al_2O_3 catalysts, *Applied Catalysis A: General*, 189, 2, (1999), 243-250 https://doi.org/10.1016/S0926-860X(99)00281-1

[15] Rodiansono Rodiansono, Muhammad Iqbal Pratama, Maria Dewi Astuti, Abdullah Abdullah, Agung Nugroho, Susi Susi, Selective Hydrogenation of Dodecanoic Acid to Dodecane-1-ol Catalyzed by Supported Bimetallic Ni-Sn Alloy, *Bulletin of Chemical Reaction Engineering & Catalysis*, 13, 2, (2018), 311-319 https://doi.org/10.9767/bcrec.13.2.1790.311-319

[16] A. P. Damayanti, H. P. Dewi, Selective hydrogenation of levulinic acid to γ -valerolactone using bimetallic Pd-Fe catalyst supported on titanium oxide, *IOP Conference Series: Materials Science and Engineering*, 2020 https://doi.org/10.1088/1757-899X/980/1/012013

[17] Rodiansono Rodiansono, Elisa Hayati, Atina Sabila Azzahra, Maria Dewi Astuti, Kamilia Mustikasari, Sadang Husain, Sutomo Sutomo, Selective

Hydrogenation of Stearic Acid to 1-Octadecanol Using Bimetallic Palladium-Tin Supported on Carbon Catalysts at Mild Reaction Conditions, *Bulletin of Chemical Reaction Engineering & Catalysis*, 16, 4, (2021), 888-903 https://doi.org/10.9767/bcrec.16.4.11895.888-903

[18] Syahrul Khairi, Takayoshi Hara, Nobuyuki Ichikuni, Shogo Shimazu, Highly efficient and selective hydrogenation of unsaturated carbonyl compounds using Ni–Sn alloy catalysts, *Catalysis Science & Technology*, 2, 10, (2012), 2139-2145 https://doi.org/10.1039/C2CY20216F

[19] Seymour Lowell, Joan E. Shields, Martin A. Thomas, Matthias Thommes, *Characterization of porous solids and powders: surface area, pore size and density*, Kluwer Academic Publisher, Dordrecht, The Netherlands., 2006, https://doi.org/10.1007/978-1-4020-2303-3

[20] Gloria Lourdes Dimas-Rivera, Javier Rivera De la Rosa, Carlos J. Lucio-Ortiz, Daniela Xulú Martínez-Vargas, Ladislao Sandoval-Rangel, Domingo Ixtcoatl García Gutiérrez, Carolina Solis Maldonado, Bimetallic Pd-Fe supported on γ -Al_2O_3 catalyst used in the ring opening of 2-methylfuran to selective formation of alcohols, *Applied Catalysis A: General*, 543, (2017), 133-140 https://doi.org/10.1016/j.apcata.2017.06.019

[21] Anne Galarneau, François Villemot, Jeremy Rodriguez, François Fajula, Benoit Coasne, Validity of the t-plot method to assess microporosity in hierarchical micro/mesoporous materials, *Langmuir*, 30, 44, (2014), 13266-13274 https://doi.org/10.1021/la5026679

[22] Emil Dumitriu, Vasile Hulea, Effects of channel structures and acid properties of large-pore zeolites in the liquid-phase *tert*-butylation of phenol, *Journal of Catalysis*, 218, 2, (2003), 249-257 https://doi.org/10.1016/S0021-9517(03)00159-3

[23] Jingjuan Wang, Petr A. Chernavskii, Ye Wang, Andrei Y. Khodakov, Influence of the support and promotion on the structure and catalytic performance of copper–cobalt catalysts for carbon monoxide hydrogenation, *Fuel*, 103, (2013), 1111-1122 https://doi.org/10.1016/j.fuel.2012.07.055

[24] Francesco Arena, Roberto Dario, Adolfo Parmaliana, A characterization study of the surface acidity of solid catalysts by temperature programmed methods, *Applied Catalysis A: General*, 170, 1, (1998), 127-137 https://doi.org/10.1016/S0926-860X(98)00041-6

[25] Nahid Khandan, Mohammad Kazemeini, Mahmoud Aghaziarati, Determining an optimum catalyst for liquid-phase dehydration of methanol to dimethyl ether, *Applied Catalysis A: General*, 349, 1-2, (2008), 6-12 https://doi.org/10.1016/j.apcata.2008.07.029

[26] Powder Diffraction File, in: Pennsylvania, USA

[27] Raghu V. Maligal-Ganesh, Chaoxian Xiao, Tian Wei Goh, Lin-Lin Wang, Jeffrey Gustafson, Yuchen Pei, Zhiyuan Qi, Duane D. Johnson, Shiran Zhang, Franklin Tao, A ship-in-a-bottle strategy to synthesize encapsulated intermetallic nanoparticle catalysts: exemplified for furfural hydrogenation, *ACS Catalysis*, 6, 3, (2016), 1754-1763 https://doi.org/10.1021/acscatal.5b02281

[28] Dmitry E. Doronkin, Sheng Wang, Dmitry I. Sharapa, Benedikt J. Deschner, Thomas L. Sheppard, Anna Zimina, Felix Studt, Roland Dittmeyer, Silke Behrens, Jan-Dierk Grunwaldt, Dynamic structural changes of supported Pd, PdSn, and PdIn nanoparticles during continuous flow high pressure direct H_2O_2 synthesis, *Catalysis Science & Technology*, 10, 14, (2020), 4726-4742 https://doi.org/10.1039/D0CY00553C

[29] Rongrong Li, Jia Zhao, Deman Han, Xiaonian Li, Pd/C modified with Sn catalyst for liquid-phase selective hydrogenation of maleic anhydride to gamma-butyrolactone, *Chinese Chemical Letters*, 28, 6, (2017), 1330-1335 https://doi.org/10.1016/j.cclet.2017.04.028

[30] Nicholas Kaylor, Jiahan Xie, Yong-Su Kim, Hien N. Pham, Abhaya K. Datye, Yong-Kul Lee, Robert J. Davis, Vapor phase deoxygenation of heptanoic acid over silica-supported palladium and palladium-tin catalysts, *Journal of Catalysis*, 344, (2016), 202-212 https://doi.org/10.1016/j.jcat.2016.09.028

[31] Gwen J. S. Dawes, Elinor L. Scott, Jérôme Le Nôtre, Johan P. M. Sanders, Johannes H. Bitter, Deoxygenation of biobased molecules by decarboxylation and decarbonylation–a review on the role of heterogeneous, homogeneous and bio-catalysis, *Green Chemistry*, 17, 6, (2015), 3231-3250 https://doi.org/10.1039/C5GC00023H

[32] Jan W. Veldsink, Martin J. Bouma, Nils H. Schöön, Antonie A. C. M. Beenackers, Heterogeneous hydrogenation of vegetable oils: a literature review, *Catalysis Reviews*, 39, 3, (1997), 253-318 https://doi.org/10.1080/01614949709353778

[33] P. Mäki-Arvela, M. Snåre, K. Eränen, J. Myllyoja, D. Yu Murzin, Continuous decarboxylation of lauric acid over Pd/C catalyst, *Fuel*, 87, 17-18, (2008), 3543-3549 https://doi.org/10.1016/j.fuel.2008.07.004